

# Using maps to predict economic activity<sup>1</sup>

Imryoung Jeong<sup>2</sup> Hyunjoo Yang<sup>3</sup>

December 1, 2021

## Abstract

We introduce a novel machine learning approach to leverage historical and contemporary maps to systematically predict economic statistics. Remote sensing data have been used as reliable proxies for local economic activity. However, they have only become available in recent years, thus limiting their applicability for long-term analysis. Historical maps, on the other hand, date back several decades. Our simple algorithm extracts meaningful features from the maps based on their color compositions. The grid-level population predictions by our approach outperform the conventional CNN-based predictions using raw map images. It also predicts population better than other approaches using night light satellite images or land cover classifications as the input for predictions.

JEL Classifications: J11, N30, R11

Keywords: historical maps, regional economic activity, machine learning

## 1. Introduction

Many important economic questions on growth and development hinge on accurate measurements of economic variables over the long run. Although remote sensing data, such as nighttime luminosity and day-time satellite images, have been used as reliable proxies for

---

<sup>1</sup> Hyunjoo Yang acknowledges research support by National Research Foundation of Korea Research Grant (Grant number: #2021069641). All errors are ours.

<sup>2</sup> Sogang University, School of Economics, Baekbeom-ro 35, Mapo-gu, Seoul, South Korea (email address: neptune0118@gmail.com).

<sup>3</sup> Sogang University, School of Economics, Baekbeom-ro 35, Mapo-gu, Seoul, South Korea (email address: hyang@sogang.ac.kr).

local economic activity, they have only become available in recent years, thus limiting their applicability for long-term analysis.

In this paper, we introduce historical and contemporary maps as a potential solution. We develop a computationally lightweight machine learning algorithm customized for using maps as inputs to generate grid-level economic proxies. We show that both current and historical maps can be used to systematically predict population density, a benchmark measure for evaluating the predictive power of remote sensing data.

Recently, researchers have measured and predicted economic variables using geospatial datasets collected from mobile phone networks (Blumenstock et al., 2015) and digital platforms (Glaeser et al., 2018), or maps of buildings (Arribas-Bel et al., 2021 ; de Bellefon et al., 2021). Henderson et al. (2012) pioneered what has become one of the most popular approaches: utilizing remotely sensed luminosity at night to measure economic growth. While nighttime luminosity has shown promising improvements in measuring economic activities (Pinkovski and Sala-i-Martin, 2016), it appears less capable in less developed countries where the provision of electricity is lacking (Jean et al., 2016).

In a growing body of research, scholars have attempted to address this challenge by combining daytime satellite imagery with machine learning approaches (Jean et al., 2016 ; Yeh et al., 2020). However, the implementation of state-of-the-art machine learning models is a significant hurdle social scientists must overcome to leverage satellite images. Moreover, nighttime luminosity and daytime satellite images hardly fill the data gap between the recent and distant past. For example, nightlight luminosity data only date back to 1992, and high-resolution satellite images covering the entire globe, including Landsat, Sentinel2, and Google Static Maps only date back to the mid-2010s.

Historical maps are probably the only alternatives to remote sensing data that date back several decades in this regard. For hundreds of years, maps have been used to effectively convey complex geographical and spatial information through abstract symbols, shapes, and text. Similar to remote sensing data, maps can provide consistent measurements across country borders. For example, the U.S. Army produced a series of 1:250,000 maps of regions covering most continents between the 1940s and the 1960s, now fully disclosed to the public (Figure 1).

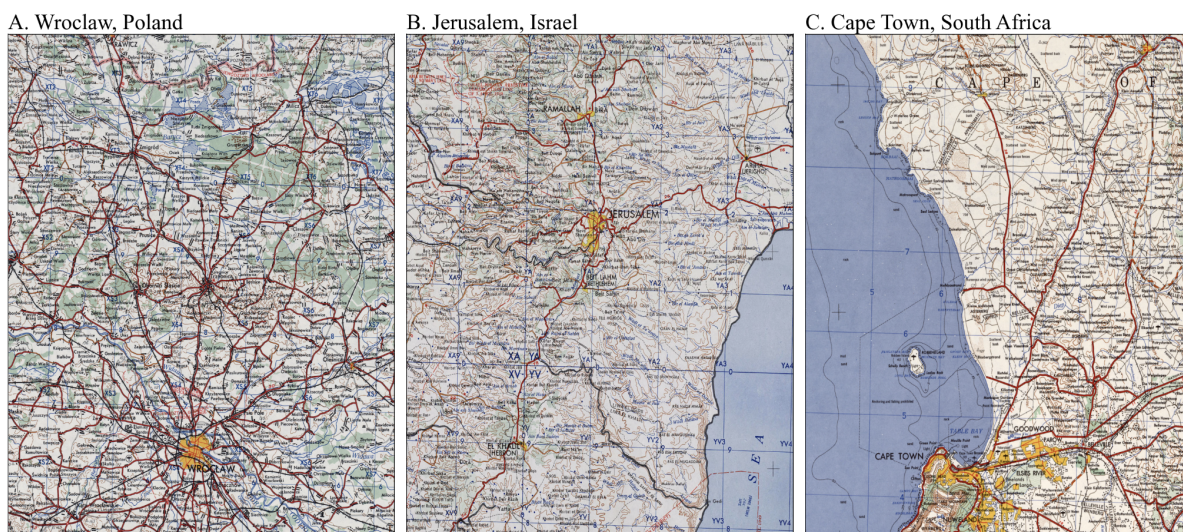


Figure 1: U.S. Army maps from different continents in the mid-20th century

Yet, it is precisely this distinct way of communicating information that prevents researchers from using historical maps. Existing machine learning models (e.g, convolutional neural networks) are almost always tuned to photographic data, such as daytime satellite images, and tend to perform poorly when applied to abstract symbols such as those found on maps.

To address this problem, we introduce a novel approach to leverage full-color topographic maps to systematically predict an economic measure across an entire country based on machine learning. Our algorithm extracts meaningful features from the maps based on their color compositions using the feature engineering aspect of machine learning. To test our approach, we digitized and georeferenced current and historical maps of most parts of South Korea from two periods half a century apart. When checked against high-quality grid-level population data from the South Korean government, our algorithm predicts population density with high accuracy after using only a small training set of approximately 2,000 images (10% of the total grids).

Another attractive characteristic of our algorithm is that it does not require heavy computational resources. We use simple machine learning models that can be run on a typical economist’s laptop or free cloud computing sources, including Google Colab: K-means clustering, linear regression model, and deep neural network model with two hidden layers. Moreover, our approach can be easily applied to different sources of input. Social scientists

with minimal knowledge of Python can readily replicate our method to predict regional economic measures by applying it to different historical maps or other spatial datasets where colors convey meaningful signals.

Another advantage of our method is flexibility in data structure of target or ground truth. A typical machine learning application using map images as input requires a label for each image. As a result, grid-level ground truth data are most suitable. Our algorithm, on the other hand, extracts meaningful features from each image and they can be easily converted into regional-level inputs so that regional-level ground truth data can be employed for predictions. Most historical data sets are available in regional-level formats, not in grid-level ones.

To the best of our knowledge, we are the first to use historical maps to systematically predict economic variables. Our research is closely related to growing literature in which scholars have used machine learning to recover historical datasets. For example, Feigenbaum, 2016 used classification algorithms to link the historical U.S. census data between 1915 and 1940, and Shen et al. (2020) applied deep learning-based layout parsers to extract information from historical Japanese documents. We make an important contribution to the literature by providing a general algorithm that can be applied to any georeferenced historical and contemporary maps to generate economic proxies. Despite their appeal, historical archives are underutilized due to the costly and labor-intensive nature of pre-processing data for analysis (see Combes et al., 2021 for the summary). We overcome this limitation by introducing a simple but effective approach that enables researchers to analyze data from full-color maps, both contemporary and historical.

More broadly, our study is related to literature in which researchers have used geospatial data to predict local economic measures such as income and assets (Jean et al., 2016) or urban areas (Baragwanath et al., 2021 ; Galdo et al., 2021). Some researchers have utilized Google Street View to measure the urban appearance and changes over time (Naik et al., 2016 ; Naik et al., 2017). Glaeser et al. (2018) showed that urban appearance can explain a considerable portion of the income levels in metropolitan areas in the United States. We contribute to this strand of literature by highlighting maps as another promising source of geospatial data that can be used to predict local economic activity.

## 2. Data and Method

The main data source is a collection of full-color topographic maps of South Korea produced in 2015 by the National Geographic Information Institute (NGII). The maps, which cover the entire nation, contain a wide range of information, including various human-built structures (e.g., buildings and road networks) as well as natural features (e.g., mountains and rivers) at a 1:50,000 scale. We georeference a total of 211 maps using the WGS84 (EPSG:4326)<sup>4</sup> coordinate system. We also georeference 214 maps in the 1970s, which are also provided by the NGII.



Figure 2: Comparisons of maps and nightlights

To assess the predictive power of maps compared to other inputs, we use two datasets as a reference. First, we utilize the harmonized version of nighttime luminosity data (*nightlights*) of 2016 by Li et al. (2020). Satellite-based nighttime light intensity is reported at a spatial resolution of 30 arc-seconds and quantified as an integer between 0 to 63, where higher numbers indicate greater light intensity. The average nighttime light intensity at the grid level is used as a one-dimensional predictor of population density (target). We also use land cover

<sup>4</sup> Jeju Island is excluded. The map for the Danyang region (code : 36802) was not available.

and land use (LCLU) at a scale of 1:50,000 provided by South Korea’s Ministry of Environment. Land cover is categorized as used area, agricultural land, forest, grass, wetland, barren, and water. We calculate the number of pixels allocated to each category and use these category counts as predictors.

**Table 1:** Descriptive Statistics

	Obs.	Mean	Median	S.D.	Min	Max
Population	27,897	1,845.54	119	9,152.49	0	152,454
Population (inhabited grids only)	22,510	2,287.20	180	10,139.32	6	152,454

The NGII also has provided georeferenced grid-level population data annually since 2014. We utilize a 2km by 2km grid with 2016 population data. Table 1 shows the descriptive statistics of the grid-level population data. The population density per  $4km^2$  has a mean of 1,839 and a standard deviation of 9,139. NGII assigns zero value to grid cells with less than 6 residents due to the confidentiality problem. The distribution of the population per grid cell is extremely skewed toward zero, with 5,469 (19.5%) grid cells having zero population. This level of skewness can largely interfere with a model’s learning; thus, we use the log of population as a prediction target. When only inhabited grid cells are included, the population density has a mean of 2,286 with a standard deviation of 10,138.

Our approach involves three main steps. First, we convert the colors on the maps into a simple, standardized color palette, thereby enabling us to compare across the maps. Then, we count the number of pixels associated with each standardized color on a map to quantify its color composition. Finally, we train a linear regression model and a deep neural network model to predict the log population using the color counts from the previous step as inputs.

Our algorithm also demonstrates the importance of the feature engineering aspect of machine learning. Feature engineering is the process of using domain knowledge about the input data and applying non-learned transformations before inputs are added to the model. Contrary to the popular conception that model development is the most important part of machine learning, experts emphasize the importance of careful pre-processing and feature engineering to prepare for high-quality input data. Simpler and more structured inputs can have a stronger

impact on improving a machine learning model’s prediction accuracy than tweaking and tuning the model itself. As an analogy, consider making an algorithm that can learn to tell the time based on images of an analog clock (Chollet, 2021). Simply using the raw images as input would be a much more computationally expensive task. However, converting each input image into two numbers representing the polar coordinates of the clock hands greatly simplifies the complexity of learning. This is the advantage of feature engineering. Through careful feature engineering, we are able to extract information from maps without applying object detection and image segmentation algorithms.

We now describe our approach in further detail.

**Pre-processing.** We clip the georeferenced topographic maps into 2 km by 2 km grid cells to match the population grids from NGII. Then, we merge the population density data with the grid cells. During the clipping and merging process, we remove grid cells located at the original maps’ borders because they contain redundant areas (e.g., descriptions), which might disturb efficient learning. We also exclude grid cells with distorted areas caused by the reprojection process of the full-sized maps. The maps are georeferenced based on WGS84 (EPSG:4326), whereas the population grids are based on the Korea 2000/Unified CS (EPSG:5179) coordinate system, so distortion due to the reprojection process is unavoidable. As a result, the final dataset used in the analysis contained 22,209 grid cells.

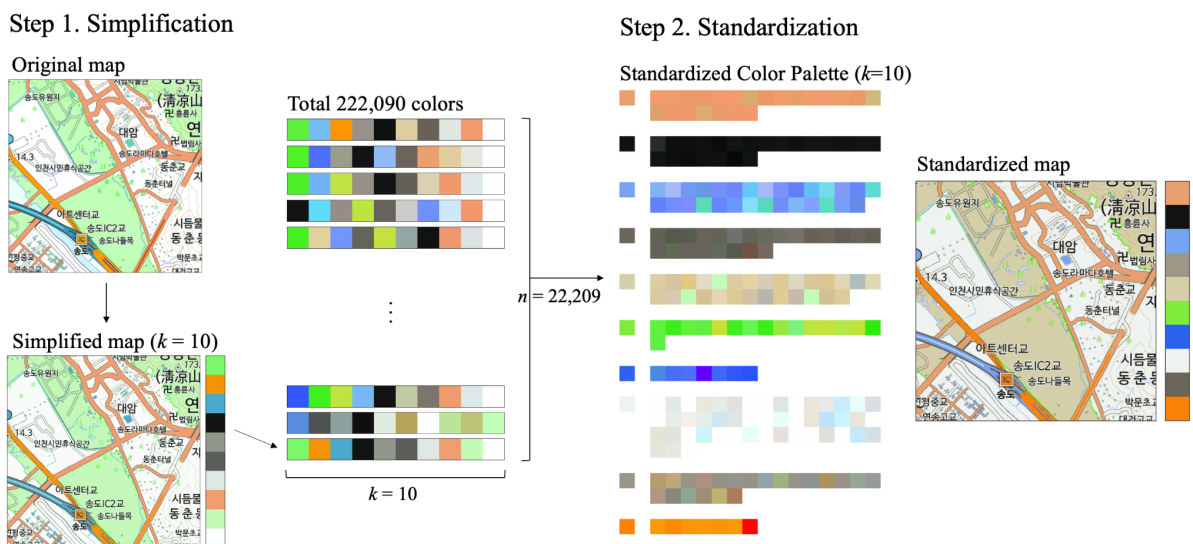


Figure 3: Our model’s approach of reducing feature dimensions in maps

**Simplification.** We simplify the color palette through the simple K-means clustering. K-means clustering algorithm classifies the data points into a fixed number of clusters ( $k$ ) without providing any guidance on how to classify them. Starting with random choices of the center of clusters (i.e., *centroids*), the algorithm allocates anonymous data points to the closest cluster based on the distance between a data point and the centroid while updating the relative locations of centroids to minimize within-cluster variation.

We categorize the colors of the pixels composing a grid cell using the K-means clustering algorithm and a tuple of R, G, B values as an anonymous data point. By setting the number of clusters to  $k$ , a grid cell is represented by only  $k$  colors. The purpose of this clustering is to simplify the grid cells to be easily used as an input for the standardization process later while minimizing information loss. A grid cell consists of approximately  $400^2$  pixels with unique R, G, B values. Aggregating the colors of every pixel at once without any simplification would yield a list of  $400^2 * 22,209$  unique R, G, B values, thereby severely increasing computational cost. Simplification using K-means clustering in this step compresses the colors to the fixed number  $k$ , reducing the length of the list to  $k * 22,209$ .

The choice of  $k$  (the number of clusters) involves a trade-off between informational richness and computational convenience. A larger  $k$  depicts a more detailed picture, but reduces the benefit of color simplification and increases computational cost. On the other hand, a smaller  $k$  might ease the computational burden but distort the information contained in the original images. We set the number of clusters to 10 so that each image could be expressed as a combination of only 10 colors.

**Standardization.** We aggregate 222,090 colors from the previous step and apply K-means clustering once again. This process aims to create  $k$  standardized colors to enable comparison across all grid cells. Unlike the previous stage, the choice of  $k$  is contingent on how well standardized colors predict population density. We assign  $k$  values from 6 to 24, and the results reported are based on  $k = 10$ . This approach is similar to Huang et al. (2021), in which they assessed the housing quality based on categorized roof colors by K-means clustering. We extract two metrics and use them as attributes to predict the population of a grid cell: the number of pixels associated with each standardized color (*color counts*) and the Herfindahl-Hirschman index (HHI). The former captures the composition of colors, reflecting



symbols on a grid-level map (e.g., roads, meadows, buildings). The latter is calculated as the squared sum of color counts and represents how concentrated or diversified the colors are within a single grid cell, capturing the complexity of an image.

**Training the models.** We train two machine learning models to predict the grid-level population. We randomly choose 10% ( $n = 2,221$ ) and 20% ( $n = 4,442$ ) of the 22,209 grid cells as training sets.

Our first approach involves using a linear regression model with a squared term. Especially, we estimate the following equation using a training set :

$$(1) \quad Pop_i = \sum_k \alpha_k n_{k,i} + \sum_k \beta_k n_{k,i}^2 + \gamma HHI_i + \varepsilon_i$$

where  $Pop_i$  is the log population of grid  $i$ ,  $n_{k,i}$  is the number of pixels in grid cell  $i$  classified as a standard color  $k$ , and  $HHI_i$  is the Herfindahl-Hirschman index of a grid cell  $i$ .

In a second approach, we train a simple deep learning model with two layers on the same training set described above. Color counts and the HHI values are used as input data. The model assumes a non-linear relationship between those inputs and the output but does not specify an explicit functional form for the relationship.

Before turning to the prediction results, we note the following. While both approaches predict the grid-level population in a given grid cell, the key difference between the two models lies in the interpretability of the parameters (or the weights in the deep learning model). The coefficients of the linear regression model are interpretable, as it simply assumes a linear relationship between the input variables and the output; if  $\alpha_k$  is positive, then one can say that the more color  $k$  appears in a grid cell, the more likely that the grid cell depicts an area with higher population density. On the other hand, the deep neural network model passes through the layers of multiplication with the weights and the non-linear transformations, thereby minimizing the differences between predicted and actual values. This complex mathematical operation makes it difficult to interpret the deep neural network architecture. In this regard, the models face a trade-off between interpretability and prediction accuracy. As shown in the following section, the deep neural network model outperforms the linear model when a smaller training set is used.

### 3. Results

In this section, we compare the performance of the two models suggested and evaluate how well they predict the population at the grid level based merely on the color composition and image complexity of map data. To compare the predictive power of the two models in a consistent way, we regress the predicted population on the actual value and report  $R^2$ .

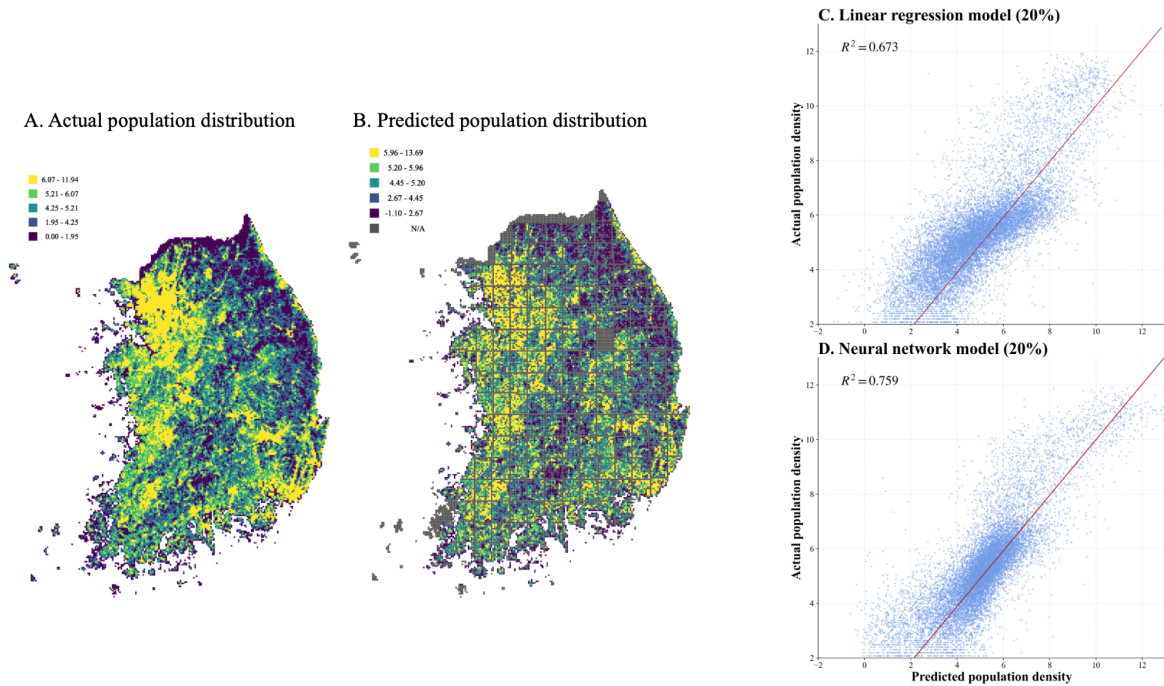


Figure 4: Actual and predicted grid-level population in 2015

Figure 4 shows the predictive performance of our models trained on 20% randomized samples when  $k = 10$ . We find that the color counts and HHI values are strongly predictive of the log population at the grid level. With a 20% training set,  $R^2$  is 0.759 for the neural network model and 0.673 for the linear regression model. These results indicate that the predictions based on color counts and HHI values can capture approximately 67% to 76% of the variation. The prediction accuracy is not much different when the models are trained using 10% of images:  $R^2$  of the neural network model decreases slightly to 0.743, while  $R^2$  of the linear regression model remains the same at 0.673.

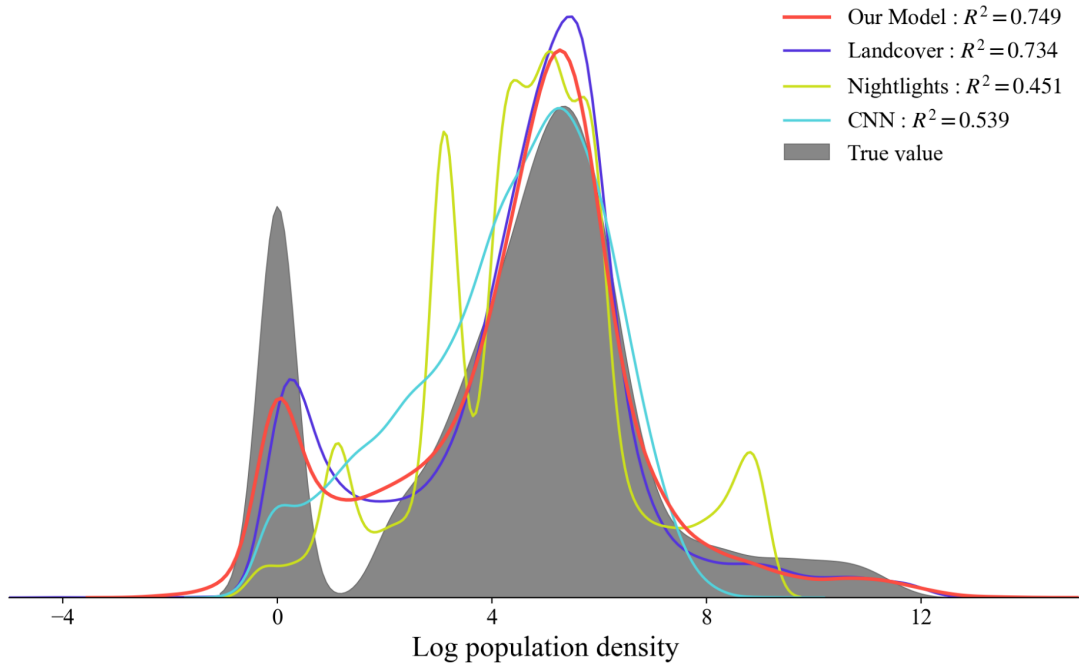


Figure 5: Kernel density plots of grid-level actual and predicted population in 2015

To evaluate the effectiveness of our approach to predict economic variables, we conduct two comparisons. First, we use nighttime luminosity and land cover classification as inputs and apply the same neural network model as points of comparison. We first calculate the average nighttime intensity and the share of land cover categories of each grid cell. Then use them to predict the log population, respectively. Second, we train the convolutional neural network model (CNN) composed of pre-trained layers of ResNet, which is widely used for computer vision problems. Then, we input the maps into the model. Note that this model does not use any features extracted from images, but rather directly uses raw images as inputs.

The results suggest that our method using maps, in which the color compositions are the feature variables, has superior predictive power. Predictions based on color counts and HHI values explain 75% of the overall variation in population density, surpassing the prediction performance of land cover (73%) and nightlights (45%). Our model shows a higher accuracy rate than the CNN counterpart which has  $R^2$  of 0.539. This result is evidence that existing

machine learning models customized to photographic images such as daytime satellite imageries might not function well with topographical maps.<sup>5</sup>

The distribution of our model’s predicted values also fits well with the distribution of true values. Figure 5 plots the kernel distribution of the predicted population density (colored lines) and the actual values (grey-colored area). The distribution plots suggest that nightlights are likely to overestimate the regions with few people and underestimate the areas with the highest population density. The structure of nighttime luminosity data can partly explain this. The night light intensity has an upper bound of 63 (i.e., top-coded), hence is not informative enough to distinguish the difference within economically active regions such as the Seoul metropolitan area. On the other hand, it has a lower bound of zero as well (i.e., bottom-censored). This characteristic makes the model less capable of predicting population density accurately, which is parallel to a limitation of night light intensity data that has recently been pointed out (Jean et al., 2016).

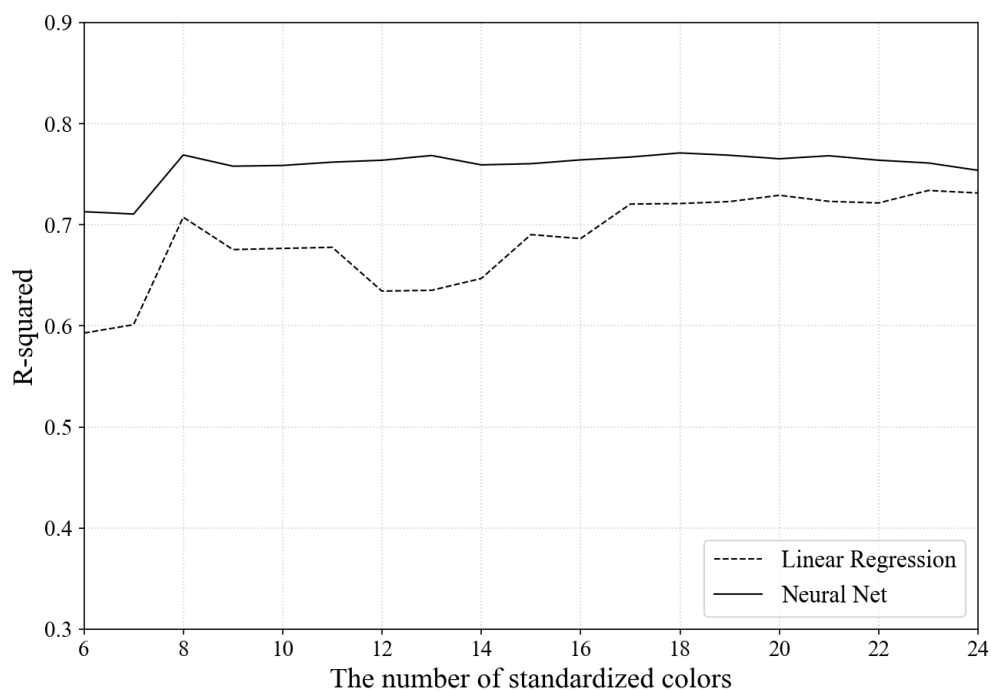


Figure 6: Prediction power and the number of standardized colors in the model

---

<sup>5</sup> We consulted machine learning experts who told us that conventional CNN is expected to perform poorly when inputs such as maps are used. Compared to photographs, maps record information in a much more complex manner. Maps include many abstract symbols and texts and contour lines often overlap each other.

Figure 6 summarizes the change in  $R^2$  based on the number of clusters selected at the standardization stage. Interestingly,  $R^2$  does not change much as  $k$  increases, and this pattern also appears when we trained our model on a 10% training set. This can be partly explained by the fact that the clusters are not cumulative; categorization does not necessarily improve as the number of clusters increases. Instead, centroids are initialized and randomly relocated, and the algorithm updates the locations of centroids to minimize the distance between them and scattered data points whenever a new  $k$  is selected. This non-cumulative nature of K-means clustering may account for the almost constant  $R^2$ .

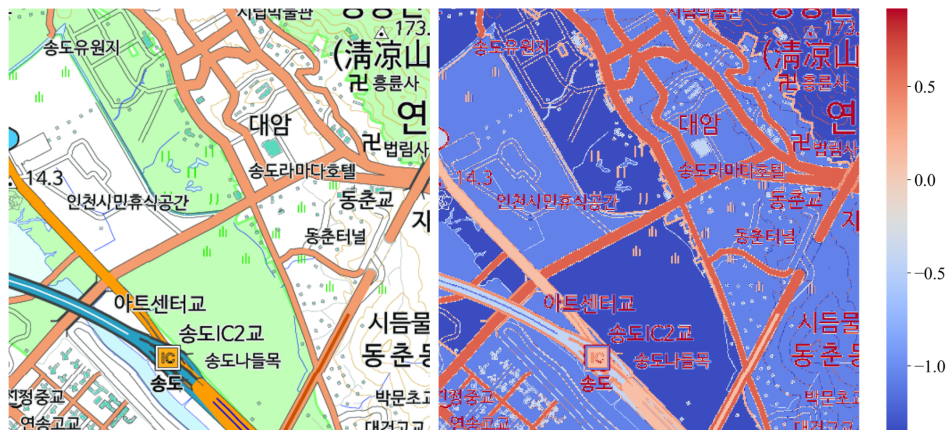


Figure 7: Interpretability of predictions

We now turn to the next exercise: disentangling the relationship between the standardized colors and the population density. We aim to understand the extent to which standardized colors play a role in predicting the population. We re-estimate the equation (1) using the predicted log population from the linear regression model with a  $k$  value of 10 as a dependent variable and combine the two coefficients,  $\alpha_k$  and  $\beta_k$ , to capture how each color does play a role in the population prediction. Figure 7 is the heatmap that visualizes the relationships between standardized colors and the predicted population, along with the original map. The combined regression coefficients are distributed along with the color lamp. The stark distinction in colors shows that human-built structures (e.g. roads, buildings, and paddies) drawn in red and natural features (e.g. mountains and rivers) drawn in blue work in the opposite direction in the population prediction. Artificial structures are positively correlated with the population density whereas natural features are negatively correlated. Because

different colors tend to be used for different symbols, this segmentation suggests that our algorithm can mimic object detection methods by capturing objects based on their colors.

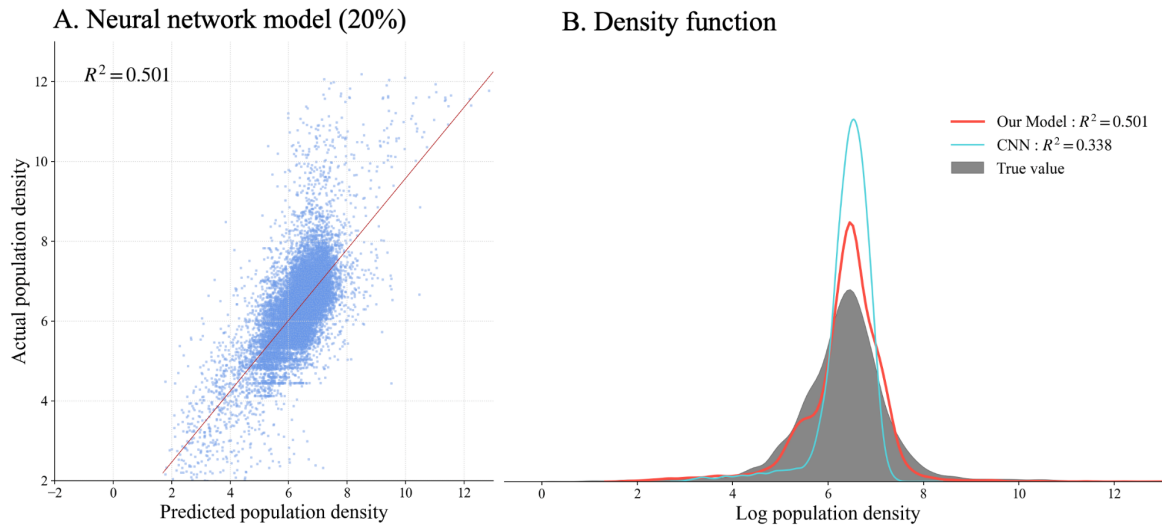


Figure 8: Actual and predicted grid-level population in 1970

We use historical maps half a century ago to verify the predictive power of our approach. We pre-process the historical maps in South Korea in the 1970s by geo-referencing and clipping them to the size of 2km by 2km grid cells. Unlike the maps in 2015, we do not have grid-level information on population density in the 1970s. Instead, we generate the population density of each cell based on town-level census population, under the assumption that population is uniformly distributed within a town. For validation, we reconstruct the grid-level population using town-level information of 2016 in the same way and compare the estimated value with the actual grid-level population density. We find that the correlation was high, 0.75.

Figure 8A visually demonstrates the correlation between predicted outcomes and actual values. Figure 8B compares the distribution of predicted values between our model and the CNN model.  $R^2$  is 0.501, which means color counts and the HHI extracted from the maps in the 1970s capture 50% of the overall variation.

The lower performance rate compared to contemporary maps can be due to several reasons. First, historical maps are paper-scanned and of lower quality. Second, the 1970 maps have far

fewer colors compared to the modern maps. Third, we generate the grid-level population based on the assumption of uniform distribution, causing measurement errors.

## 4. Conclusions

In this paper, we show that maps can be used to predict socioeconomic measures consistently. We solve the technical problem of using maps by extracting meaningful features from the complex combination of symbols, texts, and lines contained in a typical map. Our model can be applied in several ways. One application is to leverage maps with extensive spatial and temporal coverage, such as those produced by the U.S. Army Map Service<sup>6</sup> (Figure 1). In principle, our model can make a prediction on every image once they share similar color compositions with a training set. If our model is trained on a country using historically archived economic variables as labels, then it can systematically make a prediction at a granular level, even in countries lacking available historical data.

Second, our model can be applied to predict region-level economic statistics, rather than at a grid-level. Unlike existing machine learning models which require a particular type or form of inputs (e.g. CNN models use grid-level images as inputs), our model's flexibility enables us to use regional statistics as labels. This aspect is particularly important to social scientists, considering most historical data sources provide information at a regional level, such as municipalities, provinces, and counties.

A few limitations still remain. Georeferencing maps is still a labor intensive and costly prerequisite for economists to apply our model. Limited number of colors used in historical maps makes predictions noisier, particularly older maps decades ago. Yet, some possible refinements are within reach. By incorporating nation or region-wise characteristics into the model, which resembles the concept of regional fixed effects, could increase predictive power. (Park et al., 2022)

---

<sup>6</sup> <https://www.loc.gov/maps/?fa=contributor:united+states.+army+map+service>

## References

- Arribas-Bel, D., Garcia-López, M.-À., & Viladecans-Marsal, E. (2021). Building(s and) cities: Delineating urban areas with a machine learning algorithm. *Journal of Urban Economics*, *125*, 103217.
- Baragwanath, K., Goldblatt, R., Hanson, G., & Khandelwal, A. K. (2021). Detecting urban markets with satellite imagery: An application to India. *Journal of Urban Economics*, *125*, 103173.
- Blumenstock, J. E., Callen, M., Ghani, T., & Koepke, L. (2015). Promises and pitfalls of mobile money in Afghanistan: evidence from a randomized control trial. *Proceedings of the Seventh International Conference on Information and Communication Technologies and Development*, 1–10.
- Chollet, F. (2021). *Deep Learning with Python, Second Edition*. Simon and Schuster.
- Combes, P. P., Gobillon, L., & Zylberberg, Y. (2021). Urban economics in a historical perspective: Recovering data with machine learning. *Regional Science and Urban Economics*. <https://www.sciencedirect.com/science/article/pii/S0166046221000715>
- de Bellefon, M.-P., Combes, P.-P., Duranton, G., Gobillon, L., & Gorin, C. (2021). Delineating urban areas using building density. *Journal of Urban Economics*, *125*, 103226.
- Feigenbaum, J. J. (2016). *Automated census record linking: A machine learning approach*. [https://ranabr.people.stanford.edu/sites/g/files/sbiybj5391/f/machine\\_learning\\_approach.pdf](https://ranabr.people.stanford.edu/sites/g/files/sbiybj5391/f/machine_learning_approach.pdf)
- Galdo, V., Li, Y., & Rama, M. (2021). Identifying urban areas by combining human judgment and machine learning: An application to India. *Journal of Urban Economics*, *125*, 103229.
- Glaeser, E. L., Kim, H., & Luca, M. (2018). Nowcasting Gentrification: Using Yelp Data to Quantify Neighborhood Change. *AEA Papers and Proceedings*, *108*, 77–82.
- Glaeser, E. L., Kominers, S. D., Luca, M., & Naik, N. (2018). Big data and big cities: The promises and limitations of improved measures of urban life. *Economic Inquiry*, *56*(1), 114–137.
- Henderson, J. V., Storeygard, A., & Weil, D. N. (2012). Measuring economic growth from outer space. *The American Economic Review*, *102*(2), 994–1028.
- Huang, L. Y., Hsiang, S., & Gonzalez-Navarro, M. (2021). Using Satellite Imagery and Deep



- Learning to Evaluate the Impact of Anti-Poverty Programs. In *arXiv [econ.GN]*. arXiv. <http://arxiv.org/abs/2104.11772>
- Jean, N., Burke, M., Xie, M., Davis, W. M., Lobell, D. B., & Ermon, S. (2016). Combining satellite imagery and machine learning to predict poverty. *Science*, 353(6301), 790–794.
- Li, X., Zhou, Y., Zhao, M., & Zhao, X. (2020). A harmonized global nighttime light dataset 1992–2018. *Scientific Data*, 7(1), 1–9.
- Naik, N., Kominers, S. D., Raskar, R., Glaeser, E. L., & Hidalgo, C. A. (2017). Computer vision uncovers predictors of physical urban change. *Proceedings of the National Academy of Sciences of the United States of America*, 114(29), 7571–7576.
- Naik, N., Raskar, R., & Hidalgo, C. A. (2016). Cities Are Physical Too: Using Computer Vision to Measure the Quality and Impact of Urban Appearance. *The American Economic Review*, 106(5), 128–132.
- Park, S., Ahn, D., Han, S., Lee, E., Kim, D., Yang, J., Lee, S., Park, S., Kim, J., & Cha, M. (2022). Learning economic indicators by aggregating multi-level geospatial information. In *Proceedings of the Association for the Advanced of Artificial Intelligence (AAAI) 2022 Conference*.
- Pinkovskiy, M., & Sala-i-Martin, X. (2016). Lights, camera... income! Illuminating the national accounts-household surveys debate. *The Quarterly Journal of*. <https://academic.oup.com/qje/article-abstract/131/2/579/2607043>
- Shen, Z., Zhang, K., & Dell, M. (2020). A large dataset of historical Japanese documents with complex layouts. *Proceedings of the IEEE/CVF Conference on Computer Vision and Pattern Recognition Workshops*, 548–549.
- Yeh, C., Perez, A., Driscoll, A., Azzari, G., Tang, Z., Lobell, D., Ermon, S., & Burke, M. (2020). Using publicly available satellite imagery and deep learning to understand economic well-being in Africa. *Nature Communications*, 11(1), 2583.